

WAVE SCATTERING BY PERIODIC SURFACE AT LOW GRAZING ANGLES: TWO GRAZING MODE

M. I. Charnotskii

Science and Technology Corporation
and Environmental Technology Laboratory
NOAA/ERL
325 Broadway, Boulder CO 80303, USA

- 1. Introduction**
 - 2. Principal Equations and Conventional Perturbation Results**
 - 2.1 Principal Equations
 - 2.2 CP Solution in the Presence of Two Grazing Modes
 - 3. New Perturbation Expansion in the Presence of the Two Grazing Modes**
 - 3.1 Nongrazing Incidence
 - 3.2 GP Expansion for the Low-Grazing Backscatter
 - 4. Uniform Perturbation Approximation**
 - 4.1 “Natural” Form of GP Approximations
 - 4.2 Uniform Perturbation Approximations
 - 4.3 Effective Impedance and Critical Angle
 - 5. Conclusion**
- References**

1. INTRODUCTION

We discuss here the specifics of wave scattering by a plane in an average, periodic, perfectly conducting surface when two of the scattering grazing angles are small.¹ This situation includes the low-grazing backscatter case. It is of significant practical interest for ground-based

¹ A situation where there is a single grazing modes is discussed in the accompanying paper [4].

active and passive radar studies of the ocean surface, and for long-path propagation along the ocean surface.

For the finite impedance surfaces and the Dirichlet problem, both the numerical results of Barrick [1] for the periodic surface, and general analytical results of Tatarskii and Charnotskii [2, 3] predict that the continuous scattering amplitude is proportional to the small grazing angle. This result is also supported by the conventional perturbation theory.

There is however, a certain controversial aspect when a Neuman boundary condition is imposed, as presented in details in the accompanying paper [4]. This controversy is resolved in [4] for the case of a perfectly conducting grating in the presence of a single grazing mode, and it is shown that scattering amplitude is not an analytical function of the dimensionless roughness height kh and the small grazing angle α when both parameters approach zero. The present paper addresses the scattering geometry that includes two grazing modes (Littrow mounting [5]). Wave scattering by periodic surface was investigated in the extensive series of papers by Urusovskii, and Urusovskii and Mashshvili, (refs. [10–18] of [4]). However the two grazing modes situation was not discussed in any details there.

In Section 2 we introduce the necessary formalism for the one-dimensional periodic surface scattering and the principal equations of our numerical analysis. We discuss the intrinsic limitations of the Conventional Perturbation (CP) theory in the presence of two low-grazing modes, and estimate the validity domain of CP approximation.

In Section 3 we develop a new Grazing Perturbation (GP) theory that is valid in the presence of two grazing modes. We present new asymptotic formulas for the nongrazing incidence and low-grazing backscatter cases, and discuss the validity domain of the GP formulas.

In Section 4 we propose two sets of formulas that represent the Uniform Perturbation (UP) approximation, and are valid for the small roughness heights but arbitrary values of the grazing angles. We show that, unlike in the single-grazing-mode case, introduction of the effective surface impedance is not feasible in the presence of two grazing modes, but there exists a critical grazing angle that separates the validity domains of the CP and GP asymptotes.

We present an overview of our major results in the Conclusion and discuss some implications for the nonperiodic, rough surface scattering problem.

2. PRINCIPAL EQUATIONS AND CONVENTIONAL PERTURBATION RESULTS

2.1 Principal Equations

Our principal equations for the Neuman scattering problem by periodic surface were derived in [4] in the following form

$$2\nu_0\delta_{m,0} = e_m(q_0)\nu_m + i \sum_{n=-\infty}^{\infty} e_n(q_0)(k^2 - q_m q_n)p_{m-n}(\nu_m), \quad (2.1)$$

$$T_m(q_0) = -\delta_{m,0} + e_m(q_0) + \frac{i}{2\nu_m} \sum_{n=-\infty}^{\infty} e_n(q_0)(k^2 - q_m q_n)[p_{m-n}(\nu_m) - p_{m-n}(-\nu_m)]. \quad (2.2)$$

Here, $e_n(q_{0_x})$ are Fourier coefficients of the total surface field, $T_m(q_{0_x})$ is the discrete scattering amplitude, and coefficients $p_n(\pm\nu)$ are defined by:

$$\exp(\pm i\nu\eta(x)) = 1 \pm i\nu \sum_{n=-\infty}^{\infty} p_n(\pm\nu) \exp(in\kappa x), \quad (2.3)$$

where one-dimensional L -periodic heights function $\eta(x)$ is represented by the following Fourier series:

$$\eta(x) = \sum_{n=-\infty}^{\infty} \eta_n \exp(in\kappa x), \quad \kappa = \frac{2\pi}{L}, \quad (2.4)$$

$q_n = q_0 + n\kappa$, and $\nu_m^2 = k^2 - q_m^2$ are the horizontal and vertical components of the wave vectors of diffraction orders.

2.2 CP Solution in the Presence of Two Grazing Modes

The CP series for the surface fields and scattering amplitudes is presented by formulas (3.15) and (3.16) of [4]. Consider the **non-grazing incidence** first. In this case there are two scattering modes that propagate at low grazing angles in the positive and negative directions of the x axis. We denote the numbers of these modes as m^+ and m^- , accordingly. We also assume here that both ν_{m^+} and ν_{m^-} are of the same order of magnitude, but not necessarily equal to each other. The

sum at the right-hand part of formulas (3.15) and (3.16) of [4] produces two terms inversely proportional to ν_{m^+} and ν_{m^-} , which are larger than all the other terms in the sum. Therefore, the scattering amplitude for the generic mode has the following form:

$$\begin{aligned}
 T_m(q_0) &= \delta_{m,0} - 2i \frac{(k^2 - q_m q_0)}{\nu_m} \eta_m - 2\eta_{m-m^+} \eta_{m^+} \frac{(k^2 - q_m q_{m^+})(k^2 - q_{m^+} q_0)}{\nu_{m^+} \nu_m} \\
 &\quad - 2\eta_{m-m^-} \eta_{m^-} \frac{(k^2 - q_m q_{m^-})(k^2 - q_{m^-} q_0)}{\nu_{m^-} \nu_m} \quad (2.5)
 \end{aligned}$$

Similar to the single-grazing-mode case, these additional terms have the order $O(\frac{k^2 \eta^2}{\alpha_{m^\pm}})$. However, the higher-order terms behave differently here than they did for the single grazing mode case. The terms proportional to the $(\alpha_{m^\pm})^{-2}$ have the order $O(\frac{k^3 \eta^3}{\alpha_{m^+} \alpha_{m^-}})$, the terms proportional to the $(\alpha_{m^\pm})^{-3}$ have the order $O(\frac{k^4 \eta^4}{\alpha_{m^\pm}^2 \alpha_{m^\mp}})$, and so on. Hence, the CP solution is valid when

$$\alpha_{m^\pm} > k\eta. \quad (2.6)$$

This is a more restrictive condition than one for the single grazing mode case [4] in terms of both allowed heights and grazing angles. A sketch of the validity domain of the CP approximation is presented in Fig. 1.

For the grazing scattered mode, m^+ or m^- from equation (3.16) of [4] we have:

$$\begin{aligned}
 T_{m^\pm}(q_0) &= -2i \frac{(k^2 - q_{m^\pm} q_0)}{\nu_{m^\pm}} \eta_{m^\pm} \\
 &\quad - 2\eta_{m^\pm - m^\mp} \eta_{m^\mp} \frac{(k^2 - q_{m^\pm} q_{m^\mp})(k^2 - q_{m^\mp} q_0)}{\nu_{m^+} \nu_{m^-}}. \quad (2.7)
 \end{aligned}$$

This formula and an examination of the higher-order terms show that the CP solution for grazing orders is valid under the same condition (2.6). Note that the second-order in heights terms in (2.5) and (2.7) are smaller than the first-order terms under condition (2.6). They do not extend the validity domain of the first-order formulas, but probably improve the accuracy of the result.

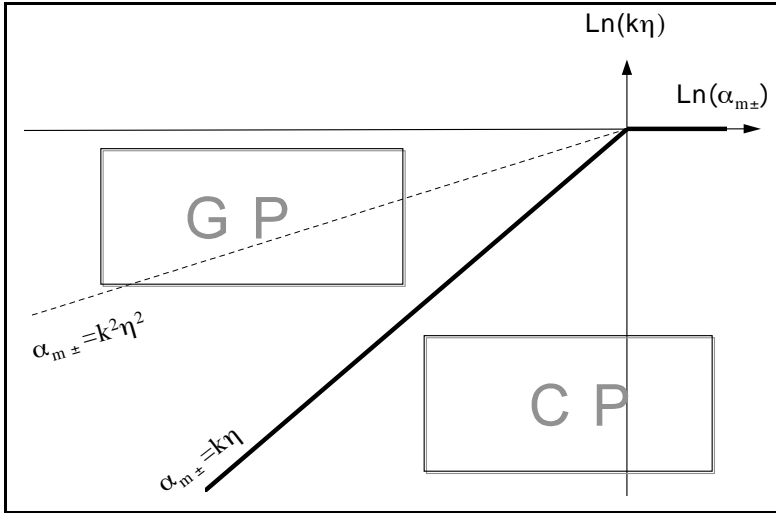


Figure 1. Validity domains of the perturbation approximations for two grazing modes.

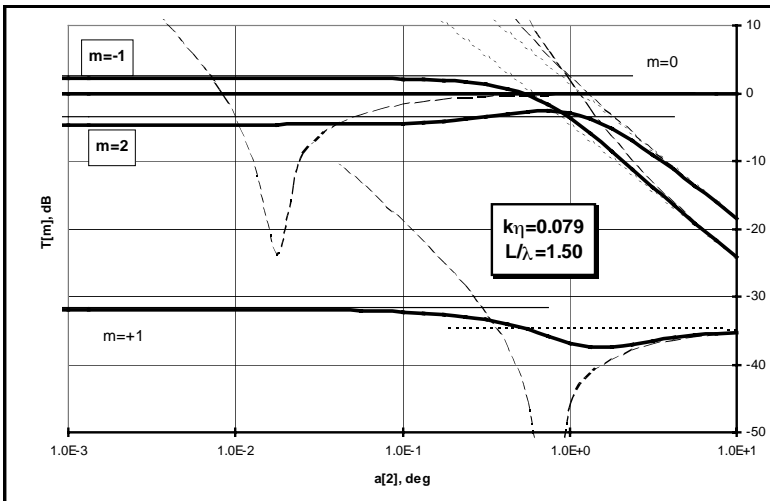


Figure 2. Scattering amplitudes for $m^+ = 2$, $m^- = -1$. Heavy solid curves – numerical solution of (2.1) and (2.2). Dotted lines – first-order perturbation results. Dashed curves – formulas (2.5) and (2.7). Light solid lines – GP formulas (3.10–3.12).

Figure 2 presents a comparison of the numerical solution of (2.1) and (2.2) and the CP formulas (2.5) and (2.7). The grazing orders are $m^+ = 2$ and $m^- = -1$. The surface period approached $L = 1.5\lambda$ and the incidence angle was close to $\alpha_0 \approx 109^\circ$ in order to keep $\alpha_2 = \alpha_{-1} \rightarrow 0$. First-order CP is quite accurate for moderate grazing angles, but fails completely at grazing even for these small heights. Second-order corrections in (2.5) and (2.7) show some accuracy improvement at moderate angles, but cause further loss of accuracy at small angles. For $k\eta = 0.079$, the critical grazing angle as given by (2.6) is about 4.5° . This matches the range where the perturbation results are close to the computation. It is also clear that all scattering amplitudes have finite limits at small grazing angles.

For the **grazing incidence**, we will keep the number $m = 0$ for the grazing specular order and use the notation $m = m^*$ for the second, nonspecular grazing order. Reciprocity allows us to avoid examination of the non-grazing scattered modes, but we still do it for the sake of convenience. The sum at the right hand part of formulas (3.15) and (3.16) of [4] contains one large term inversely proportional to α_0 . Therefore:

$$T_m(q_0) = -2i \frac{(k^2 - q_m q_0)}{\nu_m} \eta_m - 2\eta_{m-m^*} \eta_{m^*} \frac{(k^2 - q_m q_{m^*})(k^2 - q_{m^*} q_0)}{\nu_m \nu_{m^*}}, \quad m \neq 0. \quad (2.8)$$

Comparison of the second term at the right-hand part of (2.8) to the first term gives the same validity condition (2.6). This is also supported by examination of the higher-order terms.

For the grazing specular mode we have from (3.16) of [4]:

$$T_0(q_0) = 1 - 2|\eta_{m^*}|^2 \frac{(k^2 - q_0 q_{m^*})}{\nu_{m^*} \nu_0}. \quad (2.9)$$

This formula misses the $O(\frac{k\eta}{\alpha_{0,m^*}})$ terms, but we found that the next term has the order $O(\frac{k^3 \eta^3}{\alpha_{0,m^*}^3})$. Hence, the same validity condition (2.6) stands for the specular grazing mode.

For the grazing nonspecular (backscatter) mode we have:

$$T_{m^*}(q_0) = -2i \frac{(k^2 - q_{m^*} q_0)}{\nu_{m^*}} \eta_{m^*} + O\left(\frac{k^3 \eta^3}{\alpha_{m^*}^2 \alpha_0}\right). \quad (2.10)$$

The $O(\frac{k^2\eta^2}{\alpha^2})$ term is missing in this formula, but an examination of the higher-order terms shows that the CPI formula for the backscatter mode is valid under the same condition (2.6).

Figure 3 presents a comparison of the numerical solution of equations (2.1) and (2.2) and the CP formulas (2.8–2.10). The grazing orders are $m = 0$ and $m^* = -3$. When the incidence angle tends to zero, the grating period approaches $L = 1.5\lambda$ so that $\alpha_{-3} = \alpha_0$.

Similar to the single-grazing-order case [4], the reflection coefficient for the grazing mode changes its sign from $+1$ at the moderately small grazing angles to -1 when $\alpha_0 \rightarrow 0$. This is illustrated by Fig. 4, where we present the trace of the reflection coefficient $T_0(q_0)$ at the complex plane when the incidence angle changes from $\alpha_0 \approx 10^\circ$ to $\alpha_0 \approx 0.1^\circ$. Unlike in the single-grazing-mode case, there is no rotation in the complex plane. It is clear from Figs. 3 and 4 that the reflection coefficient almost vanishes at a grazing angle somewhat smaller than the critical angle (2.6), and then regains its magnitude for the smaller angles but with an opposite sign.

Figure 5 presents the magnitudes of the specular and backscattered modes for the different roughness heights. It is clear that dips in the specular amplitudes correspond to the backscatter maxima, the latest reaching the magnitude of the incident wave. The angular position of the dips is proportional to the $k\eta$ in compliance with our estimation (2.6). The width of the dips decreases for smaller heights, but their depth increases.

As a conclusion to this section we must stress that the presence of the second grazing order imposes an even more restraining requirement on the CP theory than the one revealed in [4]. Our computations as presented in Figs. 2–5 clearly indicate the existence of a distinctive domain where generic scattered orders saturate at certain levels different from the CP predictions, and the specular grazing mode amplitude changes its sign from the CP value $+1$ to -1 . The objective of the following two sections is to develop new approximations that will work for small grazing angle(s) and small heights. More specifically, we are looking for a theory that would work under condition $1 > k\eta > \alpha_{m\pm}$ when two grazing modes are present.

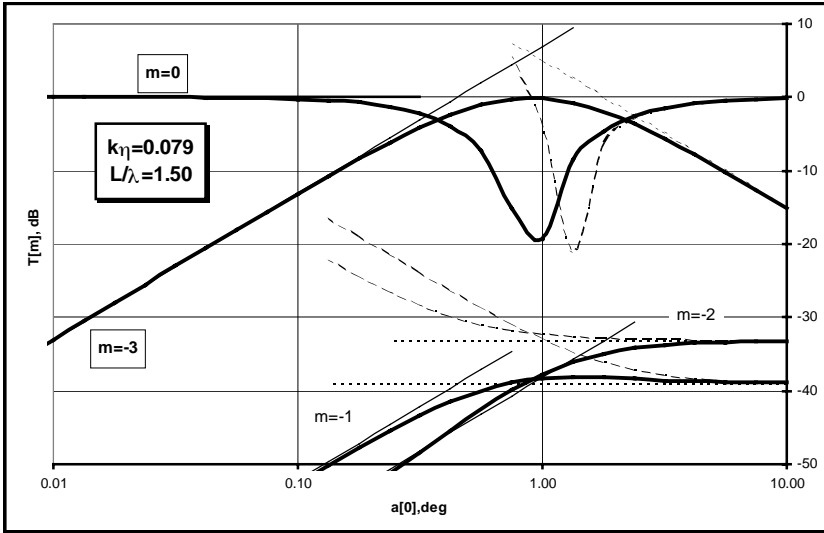


Figure 3. Scattering amplitudes for $m^* = -3$. Heavy solid curves – numerical solution of (2.1) and (2.2). Dotted lines – first-order perturbation results. Dashed curves – formulas (2.8–2.10). Light solid lines – GP formulas (3.20–3.22).

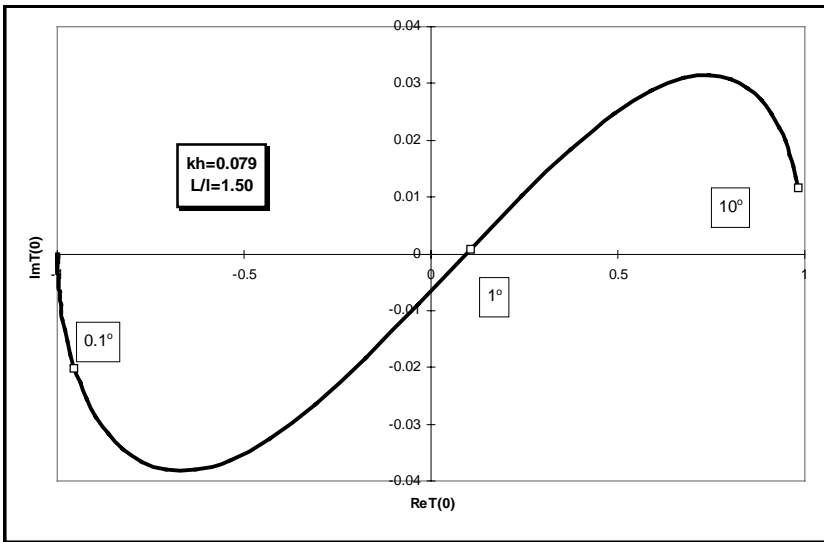


Figure 4. Complex reflection coefficient for the grazing incidence in the presence of the backscattered mode.

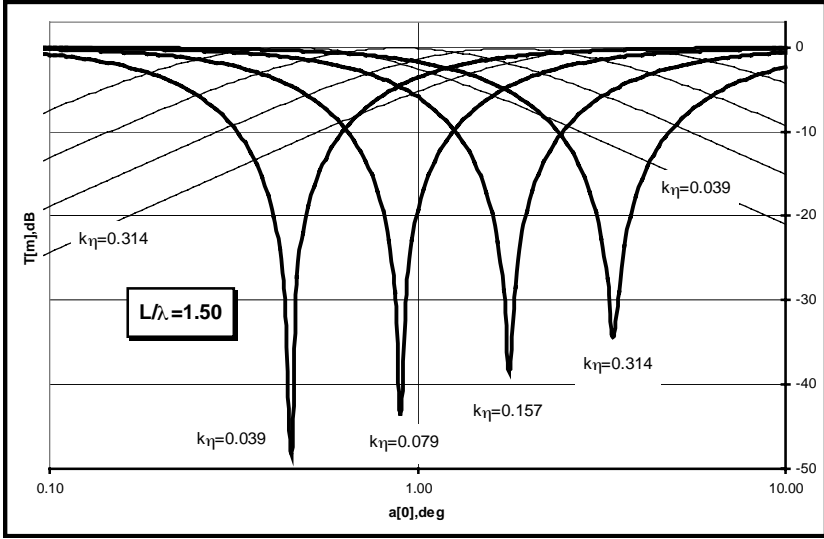


Figure 5. Magnitudes of the specular and backscattered modes. Heavy solid curves – $m = 0$, light curves – $m^* = -3$.

3. NEW PERTURBATION EXPANSION IN THE PRESENCE OF THE TWO GRAZING MODES

In this section we develop a new perturbation theory that is valid when two grazing diffraction orders are present in the spectrum of the scattered field. This expansion will be dubbed GP. It is necessary to study two individual cases: nongrazing incidence, Section 3.1, and grazing incidence, Section 3.2.

3.1 Nongrazing Incidence

Consider the case when the incident angle is not small, but there are two scattering orders, m^+ and m^- , that propagate at low grazing angles. It is clear that for this specific case under condition $\nu_{m^+}, \nu_{m^-} \ll k$ we have:

$$\kappa \approx \frac{2k}{m^+ - m^-}, \quad q_m \approx k \frac{2m - m^+ - m^-}{m^+ - m^-}. \quad (3.1)$$

We do not require here that $\nu_{m^+} = \nu_{m^-}$, but assume that $\nu_{m^-} =$

$O(\nu_{m^+})$ when $\nu_{m^+} \rightarrow 0$.

We let $\nu_{m^+} = \nu_{m^-} = 0$ in equations (2.1) for the scattering amplitudes to obtain a set of equations that carries no small parameters related to the small scattering angles:

$$\left\{ \begin{array}{l} \nu_m e_m(q_0) + ik^2 \sum_{n=-\infty}^{\infty} e_n(q_0) \\ \left[1 - \frac{(2m - m^+ - m^-)(2n - m^+ - m^-)}{(m^+ - m^-)^2} \right] p_{m-n}(\nu_m) = 2\nu_0 \delta_{m,0}, \\ \hspace{20em} m \neq m^+, m^- \\ 2ik^2 \sum_{n \neq m^+} e_n(q_0) \frac{m^+ - n}{m^+ - m^-} \eta_{m^+ - n} = 0, \\ \hspace{20em} m = m^+ \\ 2ik^2 \sum_{n \neq m^+} e_n(q_0) \frac{n - m^-}{m^+ - m^-} \eta_{m^- - n} = 0, \\ \hspace{20em} m = m^-. \end{array} \right. \quad (3.2)$$

For $k\eta \ll 1$ we can show that

$$e_m(q_0) = (\delta_{m,0} + \delta_{m,m^+} + \delta_{m,m^-}) e_m^{(0)}(q_0) + e_m^{(1)}(q_0) + \dots, \quad (3.3)$$

where $e_m^{(n)} = O(k^n \eta^n)$. We substitute (3.3) into (3.2) and keep the leading terms in $k\eta$ to obtain the following system of equations for the leading orders of $e_m(q_0)$:

$$\left\{ \begin{array}{l} \nu_0 e_0^{(0)}(q_0) = 2\nu_0 \\ 2ik^2 e_0^{(0)}(q_0) \frac{m^+}{m^+ - m^-} \eta_{m^+} + 2ik^2 e_{m^-}^{(0)}(q_0) \eta_{m^+ - m^-} = 0, \quad m = m^+ \\ 2ik^2 e_0^{(0)}(q_0) \frac{m^-}{m^+ - m^-} \eta_{m^-} - 2ik^2 e_{m^+}^{(0)}(q_0) \eta_{m^- - m^+} = 0, \quad m = m^- \\ \nu_m e_m^{(1)}(q_0) + 2ik^2 e_{m^+}^{(0)}(q_0) \frac{m^+ - m}{m^+ - m^-} \eta_{m - m^+} \\ + 2ik^2 e_{m^-}^{(0)}(q_0) \frac{m - m^-}{m^+ - m^-} \eta_{m - m^-} \\ + ik^2 e_0^{(0)}(q_0) \left[1 + \frac{(m^+ + m^-)(2m - m^+ - m^-)}{(m^+ - m^-)^2} \right] \eta_m = 0, \\ \hspace{20em} m \neq m^+, m^-. \end{array} \right. \quad (3.4)$$

The solution to (3.4) can be obtained in a straightforward manner as follows:

$$e_0^{(0)}(q_0) = 2. \quad (3.5)$$

$$e_{m^+}^{(0)}(q_0) = \frac{2m^-}{m^+ - m^-} \frac{\eta_{m^-}}{\eta_{m^- - m^+}}. \quad (3.6)$$

$$e_{m^-}^{(0)}(q_0) = \frac{-2m^+}{m^+ - m^-} \frac{\eta_{m^+}}{\eta_{m^+ - m^-}}. \quad (3.7)$$

$$\begin{aligned} e_m^{(1)}(q_0) = & -\frac{2ik^2}{\nu_m(m^+ - m^-)^2} \left\{ 2m^-(m^+ - m) \frac{\eta_{m^-} \eta_{m^- - m^+}}{\eta_{m^- - m^+}} \right. \\ & - 2m^+(m - m^-) \frac{\eta_{m^+} \eta_{m^+ - m^-}}{\eta_{m^+ - m^-}} + [(m^+ - m^-)^2 \\ & \left. + (m^+ + m^-)(2m - m^+ - m^-)] \eta_m \right\}. \end{aligned} \quad (3.8)$$

Equation (3.8) provides the leading orders for $m \neq m^+, m^-, 0$, and the first-order correction terms for $m = 0$.

When two grazing diffraction modes are present, equation (2.2) for the scattering amplitude can be written in a form that does not contain any small parameters associated with the small grazing angles:

$$\begin{aligned} T_m(q_0) = & -\delta_{m,0} + e_m(q_0) + \frac{ik^2}{2\nu_m} \sum_{n=-\infty}^{\infty} e_n(q_0) \\ & \left[1 - \frac{(2m - m^+ - m^-)(2n - m^+ - m^-)}{(m^+ - m^-)^2} \right] \left[p_{m-n}(\nu_m) \right. \\ & \left. - p_{m-n}(-\nu_m) \right]. \end{aligned} \quad (3.9)$$

Obviously, the last term at the right-hand part of (3.9) is at least of the second order in $k\eta$ when $k\eta$ is small. Hence, in order to obtain the leading terms of the scattering amplitudes in height, we only need to keep the first two terms at the right-hand part of (3.9) and use (3.5–3.8) for the surface fields. The result is:

$$T_{m^+}(q_0) = \frac{2m^-}{m^+ - m^-} \frac{\eta_{m^-}}{\eta_{m^- - m^+}}. \quad (3.10)$$

$$T_{m^-}(q_0) = \frac{-2m^+}{m^+ - m^-} \frac{\eta_{m^+}}{\eta_{m^+ - m^-}}. \quad (3.11)$$

$$\begin{aligned}
T_m(q_0) = & \delta_{m,0} - \frac{2ik^2}{\nu_m(m^+ - m^-)^2} \left\{ 2m^-(m^+ - m) \frac{\eta_{m^-} \eta_{m-m^+}}{\eta_{m^- - m^+}} \right. \\
& - 2m^+(m - m^-) \frac{\eta_{m^+} \eta_{m-m^-}}{\eta_{m^+ - m^-}} + [(m^+ - m^-)^2 \\
& \left. + (m^+ + m^-)(2m - m^+ - m^-)] \eta_m \right\}, \quad m \neq 0, m^+, m. \quad (3.12)
\end{aligned}$$

We observe that, similar to the single-grazing-mode case discussed in [4], the grazing scattering amplitudes approach a finite limit when the grazing angle tends to zero. However, the presence of the second grazing mode substantially changes the dependence of the scattering amplitudes on heights. For the generic scattered mode we now have the $O(k\eta)$ dependence compared to the $O(k^0\eta^0)$ for the single-grazing-mode case. The grazing modes themselves are $O(k^0\eta^0)$ instead of $O(k^{-1}\eta^{-1})$ as given in [4]. This decrease of the modes amplitudes agrees with the qualitative predictions of [10].

GP asymptotes (3.10–3.12) are presented as light, solid, horizontal lines at the left-hand part of Fig. 2. They appear to be very accurate for the $k\eta$ value considered.

The CP formulas (2.5) and (2.7) together with the GP formulas (3.10–3.12) form a complete set of asymptotes, but the second-order in heights terms in (2.5) and (2.7) are not mandatory. One can expect that they improve the accuracy when $1 > \alpha_{\pm} > k\eta$. However, in the vicinity of the boundary $\alpha_{\pm} \approx k\eta$ it is clear from Fig. 2 that the higher-order terms do not improve the accuracy in general.

3.2 GP Expansion for the Low-Grazing Backscatter

Consider now the case when the incidence grazing angle is small, $\nu_0 \ll k$, and the m^* -th diffraction orders is also at a low grazing angle: $\nu_{m^*} \ll k$. When the number of propagating orders $2k/\kappa$ is not large, this can happen only when the m^* -th order is close to the backscatter. We do not require here that this is exactly backscatter, or $q_m = -q_0$. We assume, however, that ν_0 and ν_{m^*} are of the same order when $\nu_0 \rightarrow 0$.

For $q_0 \approx \pm k$ we have:

$$\kappa \approx \mp \frac{2k}{m^*}, \quad q_n \approx \pm k \frac{m^* - 2n}{m^*}, \quad (3.13)$$

and equation (2.1) for the surface field can be presented in the form containing no small parameters associated with small grazing angles

besides the ν_0 at the right-hand part:

$$\left\{ \begin{array}{l} \nu_m e_m(q_0) + \frac{2ik^2}{m^*} \sum_{n=-\infty}^{\infty} e_n(q_0) \left(m + n - 2\frac{mn}{m^*} \right) p_{m-n}(\nu_m) = 0, \\ \frac{2ik^2}{m^*} \sum_{n \neq 0} e_n(q_0) n \eta_{-n} = 2\nu_0, \\ \frac{2ik^2}{m^*} \sum_{n \neq m^*} e_n(q_0) (m^* - n) \eta_{m^*-n} = 0, \end{array} \right. \quad \begin{array}{l} m \neq 0, m^* \\ m = 0 \\ m = m^*. \end{array} \quad (3.14)$$

We now seek the solution of (3.14) in the following series form:

$$e_m(q_0) = \delta_{m,m^*} e_{m^*}^{(-1)}(q_0) + e_m^{(0)}(q_0) + e_m^{(1)}(q_0) + \dots \quad (3.15)$$

This form of GP series is justified by the fact that, similar to the single-mode case in [4], the CP series (2.1) fails to accommodate equations (3.14). We also used a trial-and-error method to determine that $e_0(q_0)$ contains no terms inversely proportional to the roughness height. Eventually, all this will be justified by matching to the CP formulas and comparing with the numerical results.

We substitute (3.15) into (3.14) and keep the leading term in $k\eta$ to obtain the system of equations where each equation is homogeneous in terms of heights:

$$\left\{ \begin{array}{l} 2ik^2 \eta_{-m^*} e_{m^*}^{(-1)}(q_0) = 2\nu_0, \quad m = 0 \\ \nu_m e_m^{(0)}(q_0) + 2ik^2 \frac{(m^* - m)}{m^*} \eta_{m-m^*} e_{m^*}^{(-1)}(q_0) = 0, \quad m \neq 0, m^* \\ \eta_{m^*} e_0^{(0)}(q_0) + \sum_{n \neq 0, m^*} e_n^{(0)}(q_0) \frac{(m^* - n)}{m^*} \eta_{m^*-n} = 0, \quad m = m^*. \end{array} \right. \quad (3.16)$$

The solution of (3.16) is straightforward and the result is:

$$e_m^{(0)}(q_0) = 2 \frac{(m - m^*) \nu_0}{m^* \nu_m} \frac{\eta_{m-m^*}}{\eta_{-m^*}} \quad m \neq 0, m^*, \quad (3.17)$$

$$e_0^{(0)}(q_0) = \frac{2\nu_0}{(m^*)^2 |\eta_{m^*}|^2} \sum_{n \neq 0, m^*} \frac{(m^* - n)}{\nu_n} |\eta_{m^*-n}|^2, \quad (3.18)$$

$$e_{m^*}^{(-1)}(q_0) = -\frac{i\nu_0}{k^2 \eta_{-m}}. \quad (3.19)$$

Quite similar to the previous case, the leading terms of the scattering amplitude in heights require only the first two terms at the right-hand part of equation (2.2). The results are as follows. For any non-grazing order:

$$T_m(q_0) \approx e_m^{(0)} = 2 \frac{(m - m^*)\nu_0}{m^*\nu_m} \frac{\eta_{m-m^*}}{\eta_{-m^*}}; \quad (3.20)$$

for the grazing specular order:

$$T_0(q_0) \approx -1 + e_0^{(0)}(q_0) = -1 + \frac{2\nu_0}{(m^*)^2|\eta_{m^*}|^2} \sum_{n \neq 0, m^*} \frac{(m^* - n)}{\nu_n} |\eta_{m^* - n}|^2; \quad (3.21)$$

and for the “backscattered” order:

$$T_{m^*}(q_0) \approx e_{m^*}^{(-1)}(q_0) = \frac{-i\nu_0}{k^2\eta_{-m^*}}. \quad (3.22)$$

Note that the second term in (3.21) is of the order $O(\alpha_0)$, and is smaller than the first one. We keep it, however, in order to comply with the energy conservation principle.

It is interesting to compare the results for the grazing incidence in the presence of the grazing backscattered order (3.20–3.22) to our previous results for the grazing incidence when none of the scattered orders is near grazing: equations (4.19) and (4.20) of [4]. Similar to that earlier case, all scattering amplitudes besides the specular vanish in direct proportion to the small incidence angle, and the reflection coefficient approaches -1 when $\alpha_0 \rightarrow 0$. The height dependence is rather different, however: instead of the inverse height dependence for the generic diffraction order we see that the nongrazing orders are not dependent on the roughness height, but depend on the shape of the surface.

Numerical data for the GP asymptotes (3.20–3.22) are presented as light solid lines at the left-hand part of Fig. 3. Obviously, formulas (3.20–3.22) are very accurate at the small grazing angles. Used jointly with the first-order CP formulas (dotted lines), they can provide a reasonably good approximation for arbitrary angles for all orders besides specular, where they fail to predict the reflection “dip” discussed in detail at the end of the previous section. Incorporation of the second-order CP terms allows us to match some fine details of the $T_0(q_0)$ and $T_{-1}(q_0)$, but increases the error close to the border $\alpha_{\pm} \approx k\eta$. The accuracy of the GP asymptotes for moderate heights can be improved by including the higher order in heights terms as was discussed in [4].

Since our GP formulas for the scattering amplitude (3.10–3.12), and (3.20–3.22) are essentially rigorous expansions of the exact solution in terms of small angle and small height, one should expect that the reciprocity is preserved. A detailed check performed in [7] proved that this is actually true.

4. UNIFORM PERTURBATION APPROXIMATION

In this section we introduce a more natural form of the GP approximation that uses the real physical parameters of the problem rather than the rigorous but formal presentations obtained in Section 3. We develop uniform approximation, based on the CP and GP expansions, that is valid for small heights and arbitrary grazing angles. This uniform approximation tends toward the CP and GP results in the appropriate limits, and provide a smooth solution in the transition region between the CP and GP domains.

4.1 “Natural” Form of GP Approximations

We follow the idea discussed in Section 5.1 of [4] and replace the exact asymptote (3.12) for the generic non-grazing scattered order and **non-grazing incidence**, as follows:

$$T_m^{(q_0)} = \delta_{m,0} - \frac{2i}{\nu_m} \left[(k^2 - q_0 q_m) \eta_m - \frac{(k^2 - q_0 q_{m-})(k^2 - q_m q_{m+}) \eta_{m-} \eta_{m-m+}}{(k^2 - q_{m-} q_{m+}) \eta_{m-} \eta_{m-m+}} - \frac{(k^2 - q_0 q_{m+})(k^2 - q_m q_{m-}) \eta_{m+} \eta_{m-m-}}{(k^2 - q_{m-} q_{m+}) \eta_{m+} \eta_{m-m-}} \right]. \quad (4.1)$$

Matching this result to the CP formula (2.5) shows that at the border $\alpha_{m\pm} = O(k\eta)$ of the validity domain (2.6) for the CP theory, both (2.5) and (4.1) have the form $\delta_{m,0} + O(k\eta)$. This supports (2.6) and allows us to estimate the validity region for the GP as:

$$\alpha_{m\pm} < k\eta < 1. \quad (4.2)$$

For the grazing scattered orders and nongrazing incidence instead of (3.10) and (3.11) we have:

$$T_{m+}(q_0) = \frac{-2(k^2 - q_0 q_{m-}) \eta_{m-}}{(k^2 - q_{m-} q_{m+}) \eta_{m-} \eta_{m-m+}}, \quad (4.3)$$

$$T_{m^-}(q_0) = \frac{-2(k^2 - q_0 q_{m^+})\eta_{m^+}}{(k^2 - q_{m^+} q_{m^-})\eta_{m^+ - m^-}}. \quad (4.4)$$

The right-hand parts of (4.3) and (4.4) are of the order $O(1)$, but the CP result (2.7) is $O(\frac{k\eta}{\alpha_{m^\pm}}) + O(\frac{k^2\eta^2}{\alpha_{m^\pm}^2})$. Obviously they match at the same border $\alpha_{m^\pm} = O(k\eta)$.

The **grazing incidence** and nongrazing scatter case (3.20) can be replaced by

$$T_m(q_0) = \frac{-2\nu_0(k^2 - q_m q_{m^*})\eta_{m-m^*}}{\nu_m(k^2 - q_0 q_{m^*})\eta_{-m^*}}. \quad (4.5)$$

This formula is reciprocal to (4.3) and (4.4).

The grazing specular order in the presence of the additional scattering grazing order is now given by

$$T_0(q_0) = -1 + \frac{2\nu_0}{(k^2 - q_0 q_{m^*})^2 |\eta_{m^*}|^2} \sum_{n \neq 0, m^*} \frac{(k^2 - q_n q_{m^*})^2 |\eta_{n-m^*}|^2}{\nu_n}, \quad (4.6)$$

instead of (3.21). The right-hand part of this formula has the form $-1 + O(1)$, and should be compared to the right-hand part of (2.9) which has the form $1 + O(\frac{k^2\eta^2}{\alpha_m \alpha_0})$. At the border $\alpha_{0, m^*} = O(k\eta)$ both formulas are $O(1)$. This further supports our estimations of the validity domains for the CP and GP series, and explains the transition of the coefficient from $+1$ to -1 for the slightly rough surface at a small incidence angle.

For the grazing “backscatter” order we now have, instead of (3.22):

$$T_{m^*}(q_0) = \frac{-2i\nu_0}{(k^2 - q_0 q_{m^*})\eta_{-m^*}}. \quad (4.7)$$

The right-hand part of this formula is of the order $O(\frac{\alpha_0}{k\eta})$, and the comparable CP result (2.10) is $O(\frac{k\eta}{\alpha_{m^*}})$. They match at the border $\alpha_{0, m^*} = O(k\eta)$.

A numerical check shows that the difference between the natural and exact forms of the GP solutions is negligible in the appropriate validity domains.

4.2. Uniform Perturbation Approximations

In this section we will combine the CP solutions with the GP solutions to create a Uniform Perturbation (UP) solution, which is valid

for small heights with or without the grazing order present and reduces to the CP or GP solution when applicable.

We consider the **nongrazing incidence** first, and assume that two grazing modes are present with the numbers m^+ and m^- . Following the idea of section 5.2 of [4], we retain in the exact equation set (2.1) the terms that have been kept in the CP equations (3.17) of [4] or in the GP equations (3.4) of the present paper. The result is the following set of equations for the UP approximation:

$$\left\{ \begin{array}{l} \nu_0 e_0(q_0) = 2\nu_0, \quad m = 0, \\ \nu_{m^+} e_{m^+}(q_0) + i(k^2 - q_{m^+} q_0) \eta_{m^+} e_0(q_0) \\ \quad + i(k^2 - q_{m^+} q_{m^-}) \eta_{m^+ - m^-} e_{m^-}(q_0) = 0, \quad m = m^+, \\ \nu_{m^-} e_{m^-}(q_0) + i(k^2 - q_{m^-} q_0) \eta_{m^-} e_0(q_0) \\ \quad + i(k^2 - q_{m^-} q_{m^+}) \eta_{m^- - m^+} e_{m^+}(q_0) = 0, \quad m = m^-, \\ \nu_m e_m(q_0) + i(k^2 - q_m q_0) \eta_m e_0(q_0) + i(k^2 - q_m q_{m^-}) \eta_{m - m^-} e_{m^-}(q_0) \\ \quad + i(k^2 - q_m q_{m^+}) \eta_{m - m^+} e_{m^+}(q_0) = 0, \quad m \neq m^-, m^+. \end{array} \right. \quad (4.8)$$

The solution to this equation set can be readily obtained by the standard substitution technique. The last equation in (4.8) for $m = 0$ is also used as a correction for the $e_0(q_0) = 2$ solution of the first equation of (4.8). We substitute these surface field components into the equation (2.2) for the scattering amplitudes, where in fact only the first two terms should be retained, to obtain the scattering amplitudes in the following form:

$$T_{m^+}(q_0) = -2i \frac{[\nu_{m^-} (k^2 - q_{m^+} q_0) \eta_{m^+}]}{\nu_{m^+} \nu_{m^-} + (k^2 - q_{m^+} q_{m^-})^2 |\eta_{m^+ - m^-}|^2} - \frac{[i(k^2 - q_{m^+} q_{m^-}) (k^2 - q_{m^-} q_0) \eta_{m^+ - m^-} \eta_{m^-}]}{\nu_{m^+} \nu_{m^-} + (k^2 - q_{m^+} q_{m^-})^2 |\eta_{m^+ - m^-}|^2}. \quad (4.9)$$

$$T_{m^-}(q_0) = -2i \frac{[\nu_{m^+} (k^2 - q_{m^-} q_0) \eta_{m^-}]}{\nu_{m^+} \nu_{m^-} + (k^2 - q_{m^+} q_{m^-})^2 |\eta_{m^+ - m^-}|^2} - \frac{[i(k^2 - q_{m^-} q_{m^+}) (k^2 - q_{m^+} q_0) \eta_{m^- - m^+} \eta_{m^+}]}{\nu_{m^+} \nu_{m^-} + (k^2 - q_{m^+} q_{m^-})^2 |\eta_{m^+ - m^-}|^2}. \quad (4.10)$$

$$T_0(q_0) = 1 - \frac{i}{\nu_0} [T_{m^-}(q_0) (k^2 - q_0 q_{m^-}) \eta_{-m^-} + T_{m^+}(q_0) (k^2 - q_0 q_{m^+}) \eta_{-m^+}]. \quad (4.11)$$

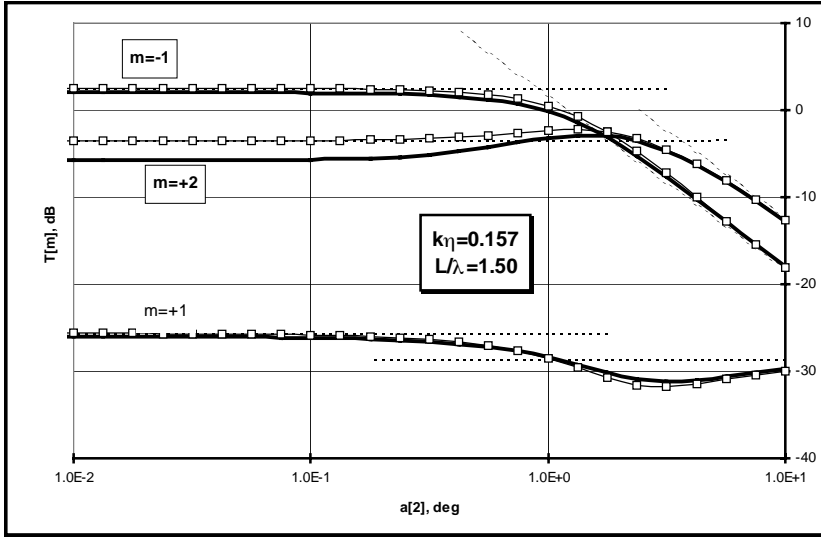


Figure 6. Comparison of the UP approximation to numerical solution for $m^+ = +2$, $m^- = -1$ and $k\eta = 0.157$. Heavy solid curves – numerical data. Dashed curves – CP and GP results. Light solid curves marked with squares – UP approximation.

$$T_m(q_0) = -\frac{i}{\nu_m} [2(k^2 - q_m q_0) \eta_m + T_{m^-}(q_0)(k^2 - q_m q_{m^-}) \eta_{m-m^-} + T_{m^+}(q_0)(k^2 - q_m q_{m^+}) \eta_{m-m^+}], \quad m \neq 0, m^-, m^+. \quad (4.12)$$

When $k\eta < \alpha_{m^\pm}$, these formulas give all the terms retained in the CP formulas (2.5) and (2.7). When $k\eta > \alpha_{m^\pm}$ they tend toward (3.10–3.12) or the “natural” forms of these formulas (4.1), (4.3) and (4.4), as expected. It is also clear from (4.9–4.12) that the transition region between these two extreme cases corresponds to $\alpha_{m^\pm} = O(k\eta)$. This matches our previous estimation (2.6).

Numerical data presented in Fig. 6 show that UP provides a smooth transition between the CP and GP asymptotes. The UP is accurate in the transition region $\alpha_{m^\pm} = O(k\eta)$ between the CP and GP where neither of the former is valid. As was noted in [4] for the single-mode case, the inaccuracy of UP is related mostly to the offshoot of the GP asymptotes for certain modes, and disappears at smaller heights. It

can be corrected if higher-order in heights GP terms are taken into account.

For the **grazing incidence** in the presence of the two grazing modes: $m = 0$ (specular) and $m = m^*$ (backscatter), equation set that combines the major terms of the conventional perturbation equation (3.17) of [4] and the GP equation (3.16) of this paper has the following form:

$$\begin{cases} \nu_0 e_0(q_0) + i(k^2 - q_0 q_{m^*}) \eta_{-m^*} e_{m^*}(q_0) = 2\nu_0, & m = 0, \\ \nu_{m^*} e_{m^*}(q_0) + i(k^2 - q_{m^*} q_0) \eta_{m^*} e_0(q_0) = 0, & m = m^*, \\ \nu_m e_m(q_0) + i(k^2 - q_m q_0) \eta_m e_0(q_0) \\ \quad + i(k^2 - q_m q_{m^*}) \eta_{m-m^*} e_{m^*}(q_0) = 0, & m \neq 0, m^*. \end{cases} \quad (4.13)$$

The second term at the left-hand part of the last equation in (3.16) is mostly responsible for the higher-order corrections to the specular reflection coefficient that are similar to (3.21). These corrections are important to keep up with the energy balance. However, in this specific case we are more interested in the transition of the specular reflection coefficient from the typical CP value $+1$ to the GP value -1 . Therefore, for the sake of simplicity, we excluded the second term at the left-hand part of the last equation in (3.16) for the derivation of (4.13). This term in principle can be included, but it complicates the final formulas significantly.

The solution of (4.13) for the surface fields can be readily obtained, and after substitution in the formula (2.2) for the scattering amplitudes we have:

$$T_0(q_0) = \frac{\nu_0 \nu_{m^*} - (k^2 - q_0 q_{m^*})^2 |\eta_{m^*}|^2}{\nu_0 \nu_{m^*} + (k^2 - q_0 q_{m^*})^2 |\eta_{m^*}|^2}, \quad (4.14)$$

$$T_{m^*}(q_0) = \frac{-2i\nu_0(k^2 - q_0 q_{m^*})\eta_{m^*}}{\nu_0 \nu_{m^*} + (k^2 - q_0 q_{m^*})^2 |\eta_{m^*}|^2} \quad (4.15)$$

$$\begin{aligned} T_m(q_0) &= \frac{[-2i\nu_0[\nu_{m^*}(k^2 - q_0 q_m)\eta_m]]}{\nu_m[\nu_0 \nu_{m^*} + (k^2 - q_0 q_{m^*})^2 |\eta_{m^*}|^2]} \\ &\quad - \frac{[i(k^2 - q_m q_{m^*})(k^2 - q_{m^*} q_0)\eta_{m-m^*}\eta_{m^*}]}{\nu_m[\nu_0 \nu_{m^*} + (k^2 - q_0 q_{m^*})^2 |\eta_{m^*}|^2]}. \end{aligned} \quad (4.16)$$

Formula (4.16) is reciprocal to either (4.9) or (4.10). Formula (4.15) is self-reciprocal, as expected.

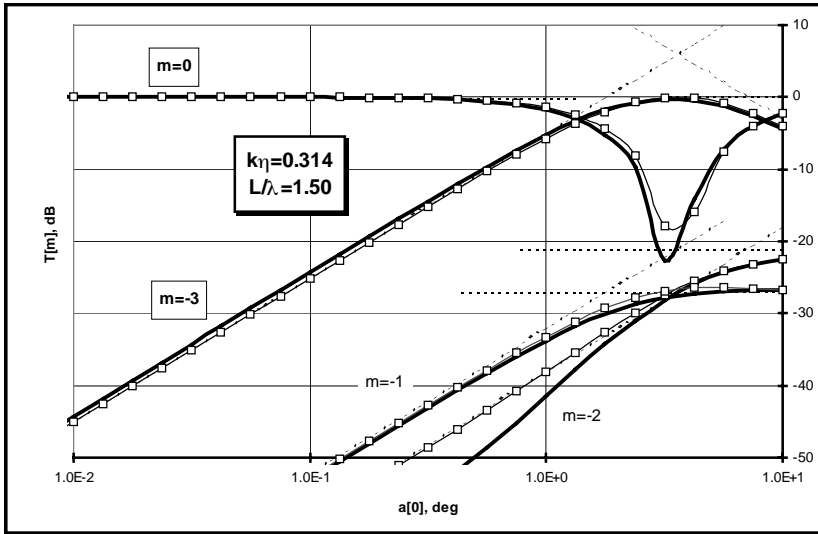


Figure 7. Comparison of the UP approximation to numerical solution for grazing incidence, $m^* = -3$, and $k\eta = 0.314$. Heavy solid curves – numerical data. Dashed curves – CP and GP results. Light solid curves marked with squares – UP approximation.

When $k\eta < \alpha_{0,m^*}$ formula (4.14) reduces to the CP result (2.9), (4.15) gives the major term of (2.10), and (4.16) gives both terms of (2.8). When $k\eta > \alpha_{0,m^*}$ formula (4.14) gives the major term of (3.21) or (4.6). The correction terms are not reproduced due to the simplifications we mentioned earlier. Formula (4.15) reduces to (3.22) and (4.7), and formula (4.16) approaches (3.20) and (4.5).

UP approximation (4.14–4.16) is compared to the numerical results, CP and GP formulas in Fig. 7. We had to use relatively large heights, $k\eta = 0.314$, in order to show the differences between UP and an exact solution for the most interesting forward- and backward- scattered modes. UP formulas are fairly accurate in the region of the dip of the reflection coefficient and the maximum of the backscattered field where neither CP nor GP formulas are valid.

4.3 Effective Impedance and Critical Angle

At first glance at UP formulas (4.9–4.12) and (4.14–4.16), one is tempted to introduce the effective impedance for this grazing incidence/backscatter case as follows:

$$Z_{EFF} = \frac{(k^2 - q_{m^+}q_{m^-})^2}{k\nu_{m^+}} |\eta_{m^+-m^-}|^2, \quad (4.17)$$

and present the reflection coefficient similar to that of the single-mode case (5.16) in [4] as follows:

$$T_0(q_0) = \frac{\nu_0 - kZ_{EFF}}{\nu_0 + kZ_{EFF}}. \quad (4.18)$$

However, this effective impedance tends to infinity when $\alpha_{m^+} \rightarrow 0$ and the Brewster angle does not exist. As we have seen before, the critical angle for this case is $\alpha_{m^*} = O(k\eta)$, and it appears that the idea of the effective impedance is not valid here. It is possible, however, to introduce the more accurate definition of the critical angle as follows:

$$\sin \alpha_C \approx \alpha_C = \frac{(k^2 - q_{m^+}q_{m^-})|\eta_{m^+-m^-}|}{k} \approx 2k|\eta_{m^+-m^-}|. \quad (4.19)$$

At this angle two components of the denominators of (4.14–4.16) are equal. For our surface model and $k\eta = 0.314$ we have $\alpha_C = 3.6^\circ$. This number agrees with the position of the dips in Fig. 7. It is noteworthy that in the continuous Fourier transform space the Fourier coefficient $\eta_{m^+-m^-}$ corresponds to the $\tilde{\eta}(2k)$, which is the component supporting propagation of surface waves.

The most interesting feature of the low-grazing forward scattering is the sign inversion of the reflection coefficient. Figure 8 presents the quadratic components of the $T_0(q_0)$ calculated numerically and according to the UP formula (4.14). UP formulas appear to be fairly accurate, even for the moderate heights, and predict correct saturation levels for the reflection coefficient. Unlike the single-grazing-order case [4], the transition of the reflection coefficient from +1 to -1 is not a rotation at the complex plane. The reflection coefficient progresses from +1 to -1 mostly along the real axis. This causes the magnitude of the reflection to almost vanish at the incidence angles close to the critical angle. In this situation the energy flux is picked up by the

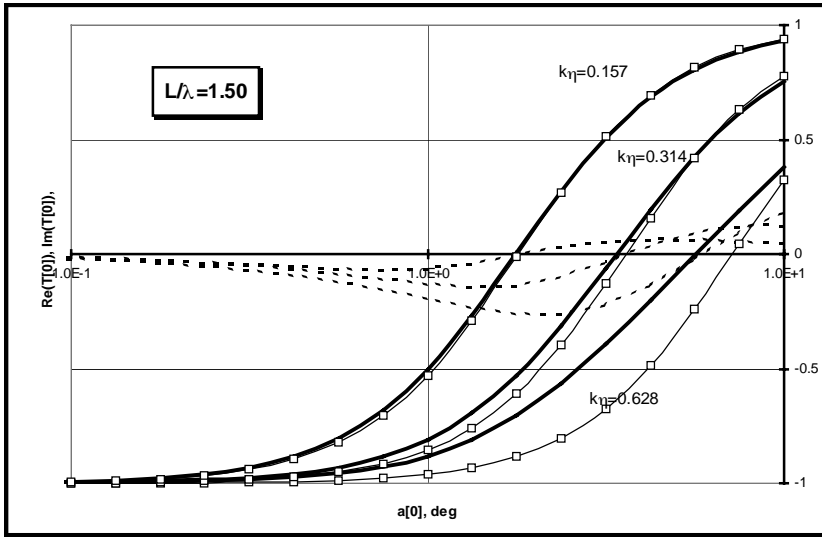


Figure 8. Complex reflection coefficient in the presence of the backscattered mode. Solid curves – real part, dashed curves – imaginary part. Heavy curves – numerical results. Curves marked by squares – UP approximation.

backscattered mode. Note that the reflection coefficient for the UP is a real number.

5. CONCLUSION

We found that for the Neuman periodic surface with a finite number of propagating scattered modes, the conventional perturbation theory is invalid when two modes propagate at a low grazing angle.

A new perturbation theory was developed that is valid when the grazing angles tend to zero and heights are small in the wavelength scale. The height dependence of these new formulas is highly nonlinear.

New perturbation theory, together with conventional perturbation theory, form a complete set of asymptotes for the scattering amplitudes when heights are small in the wavelength scale.

We found that in the presence of two grazing modes, including the low-grazing backscatter, the introduction of the effective surface

impedance is not feasible, but there exists a critical angle separating the CP and GP solutions. This development resolves the contradiction between the low-grazing backscattering results by Barrick [1] and Tatarskii/Charnotskii [2, 3] for a periodic surface case.

The critical angle is proportional to the Fourier component of heights supporting propagation of the surface wave. In our opinion this implies that the surface waves, which are allowed in the two-grazing mode propagation scenario, play the major role in restraining the amplitudes of the grazing modes. For the single-grazing-order case [4] such surface waves are prohibited, and the amplitude of the grazing mode is restricted by the multiple scattering in all other modes. The collective effect of this scattering is presented by the effective surface impedance.

We developed a uniform perturbation theory that combines the conventional and new perturbation formulas and is valid for small heights with or without the grazing modes present.

Uniform perturbation theory describes a smooth transition of the reflection coefficient for the slightly rough Neuman surface from the value of $+1$ – for the incidence angles larger than the critical angle to the value of -1 – for incidence angles smaller than the critical angle.

The sign inversion of the reflection coefficient in the presence of the two grazing modes is associated with the sharp reduction of its magnitude in the vicinity of the critical angle. At the same time the backscatter coefficient increases to the unit magnitude.

Transition to the aperiodic rough surface requires expansion of the surface period, and allows the surface to have a dense spectrum, which should include a $\tilde{\eta}(2k)$ component supporting surface waves. In our opinion the present two-grazing-modes-scenario seems to be more appropriate for this transition than the single-mode geometry of [4]. In addition to the comments presented in [4], this makes even more arguable the theory of [8–10], which relies on the intrinsic surface impedance.

ACKNOWLEDGMENTS

This document has been generated as part of a joint NOAA/DOD – Advanced Sensor Application Program. The author thanks V. I. Tatarskii, I. M. Fuks, A. G. Voronovich, and V. U. Zavorotny for their helpful comments.

REFERENCES

1. Barrick, D. E., "Grazing angle behavior of scatter and propagation above any rough surface," *IEEE Trans. Antennas Propag.*, Vol. 46, 73–83, 1998.
2. Tatarskii, V. I., and M. I. Charnotskii, "On the universal behavior of scattering from a rough surface for small grazing angles," *IEEE Trans. Antennas Propag.*, Vol. 46, 67–72, 1998.
3. Tatarskii, V. I., and M. I. Charnotskii, "Universal behavior of scattering amplitudes for scattering from a plane in average rough surface for small grazing angles," *Waves in Random Media*, Vol. 8, 29–40, 1998.
4. Charnotskii, M. I., "Wave scattering by periodic surface at low grazing angles: two grazing modes," *J. Electromagn. Waves Appl.*, 1999, (accompanying paper).
5. Hutley, M. C., *Diffraction Gratings*, Academic Press, London, New York, Ch. 6, 1982.
6. Urusovskii, I. A., "Diffraction of sound on a periodically uneven and inhomogeneous surface," *Soviet Physics-Doklady*, Vol. 5, 345–348, 1960.
7. Charnotskii, M. I., "Wave scattering at low grazing angles: New perturbation theory," *NOAA Tech. Memo*, ERL ETL-291, 1998.
8. Bass, F. G., and I. M. Fuks, *Wave scattering from statistically rough surfaces*, Pergamon Press, New York, Ch. 2, 1979.
9. Fuks, I. M., and V. I. Tatarskii, "Scattering cross-section from a rough surface for small grazing angles," *Proc. IGARSS*, IV, 2279–2283, Seattle, 1998.
10. Fuks, I. M., V. I. Tatarskii, and D. E. Barrick, "Behavior of scattering from a rough surface at small grazing angles," *Waves in Random Media*, 1999 (in press).